

Supporting Information for:

**Synthesis, Spectroscopy and Hydrogen/Deuterium
Exchange in High-Spin Iron(II) Hydride Complexes**

*Thomas R. Dugan, Eckhard Bill, K. Cory MacLeod, William W. Brennessel and Patrick L. Holland**

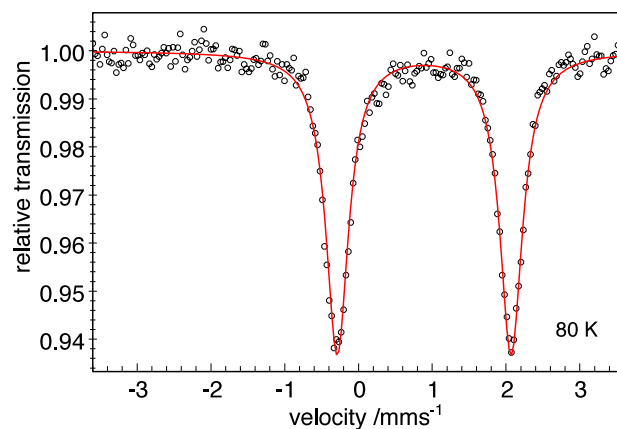


Figure S-1. Zero-field Mössbauer spectrum of $L^{\text{Me}}\text{FeBr}(\text{THF})$ (**2**) recorded at 80 K. The black circles are the data, and the red line is a simulation of the spectrum using the parameters in the text.

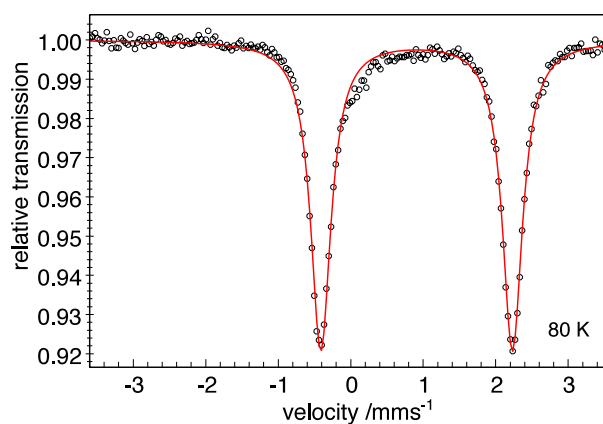


Figure S-2. Zero-field Mössbauer spectrum of $[\text{L}^{\text{Me}}\text{Fe}(\mu\text{-Br})]_2$ at 80 K. The black circles are the data, and the red line is a simulation of the spectrum using the parameters in the text.

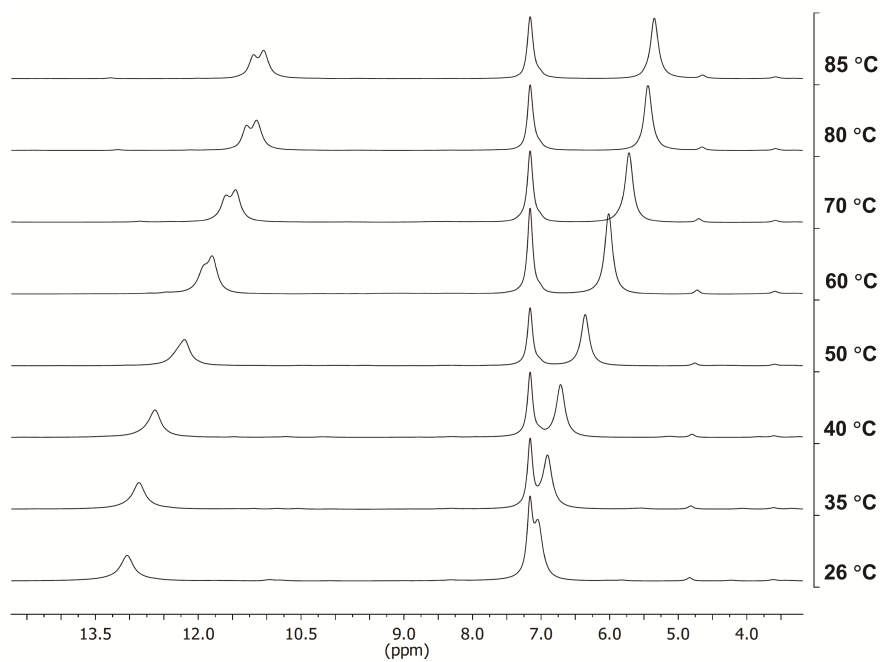


Figure S-3. Variable temperature ¹H NMR spectra of [L^{Me}Fe(μ-H)]₂ (**3**) between 26 °C and 85 °C in C₆D₆ are shown. The emergence of a peak from under the residual solvent is evident.

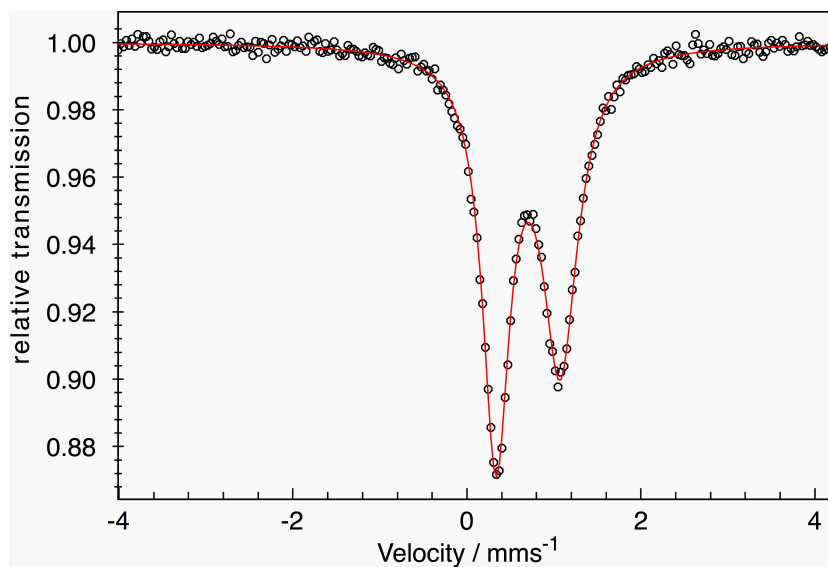


Figure S-4. Zero-field Mössbauer spectrum of independently synthesized $L^{\text{Me}}\text{Fe}(\text{C}_6\text{H}_6)$, which is known [Smith, J. M.; Sadique, A. R.; Cundari, T. R.; Rodgers, K. R.; Lukat-Rodgers, G.; Lachicotte, R. J.; Flaschenriem, C. J.; Vela, J.; Holland, P. L. *J. Am. Chem. Soc.* **2006**, *128*, 756] but not previously studied by Mössbauer spectroscopy. $\delta = 0.70$ mm/s, $|\Delta E_Q| = 0.74$ mm/s.

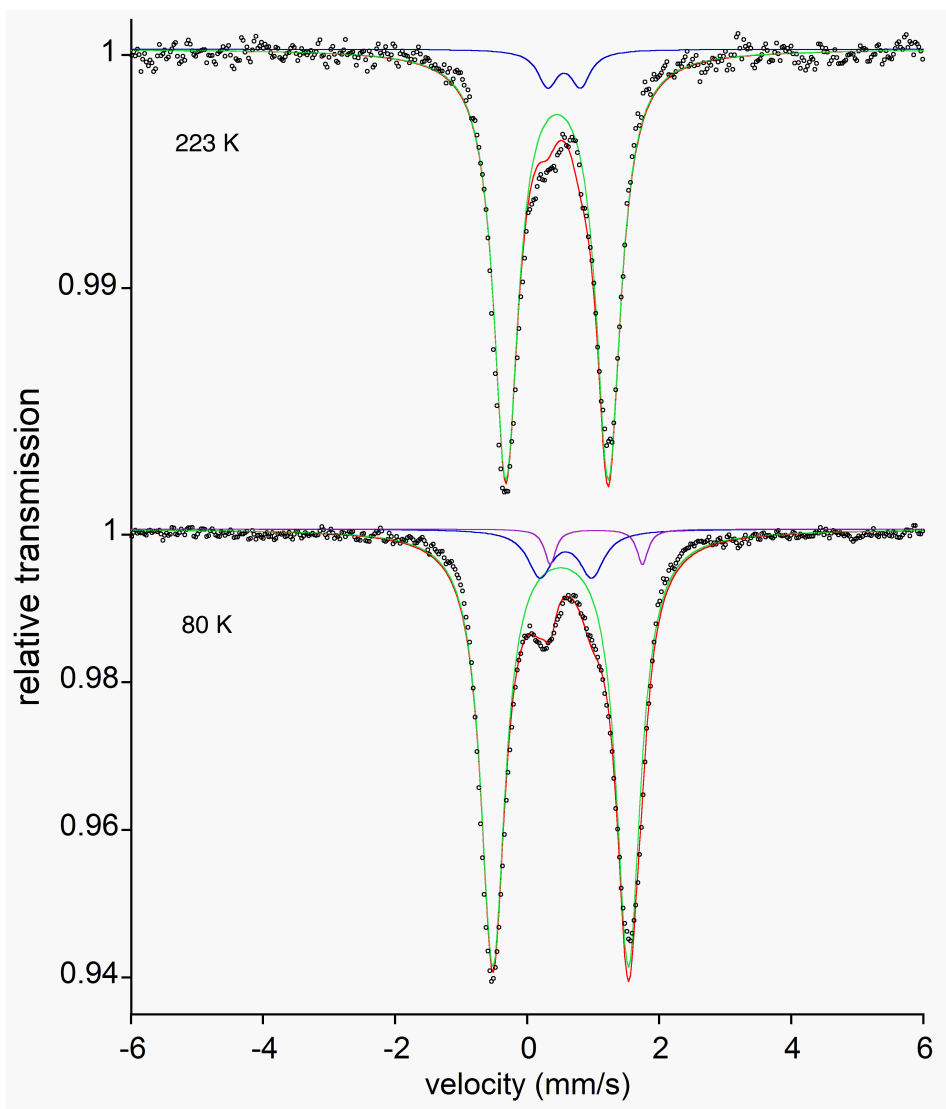


Figure S-5. Mössbauer spectra of $[\text{L}^{\text{Me}}\text{Fe}(\mu\text{-H})]_2$ (**3**) at 80 K (a) and 223 K (b). The black circles are the data and the red lines represent the sums of a major doublet for **3** (green) and unknown impurities (blue and purple). At 80 K, compound **3** has $\delta = 0.51$ mm/s and $|\Delta E_Q| = 2.05$ mm/s accounting for 87% of the sample. The minor components account for a combined 13% of the sample with (blue) $\delta = 0.59$ mm/s and $|\Delta E_Q| = 0.78$ mm/s, and (purple) $\delta = 1.05$ mm/s and $|\Delta E_Q| = 1.40$ mm/s. At 223 K, compound **3** has $\delta = 0.45$ mm/s and $|\Delta E_Q| = 1.56$ mm/s accounting for 94% of the sample (minor component of 6% has $\delta = 0.56$ mm/s and $|\Delta E_Q| = 0.50$ mm/s). The observed increase in experimental isomer shift (δ) of **3** at 80 K (as compared to 223 K) is a result of the second-order Doppler shift, which always increases δ with decreasing temperatures.[Gütlich, P.; Bill, E.; Trautwein, A. X. *Mössbauer Spectroscopy and*

Transition Metal Chemistry; Springer Verlag: Berlin, 2011.] The change in quadrupole splitting of the main doublet is less systematically predictable, but is typical when excited spin-orbit states within the ground-state manifold are populated at higher temperatures.

The key observation is that a single impurity does not adequately fit both the high- and low-temperature spectra. Thus, it is likely that the minor peaks reflect several small impurities, whose doublets are small and overlapped, preventing confident assignment. As discussed in the text, one main impurity is likely to be $L^{\text{Me}}\text{Fe}(\eta^6\text{-C}_6\text{H}_6)$, and others are likely to correspond to very small peaks observed in ^1H NMR spectra (*e.g.* Figure 7).

The 6% impurity doublet in **3-D₂** (Figure 5 of text) has $\delta = 0.67$ mm/s and $|\Delta E_Q| = 0.93$ mm/s.

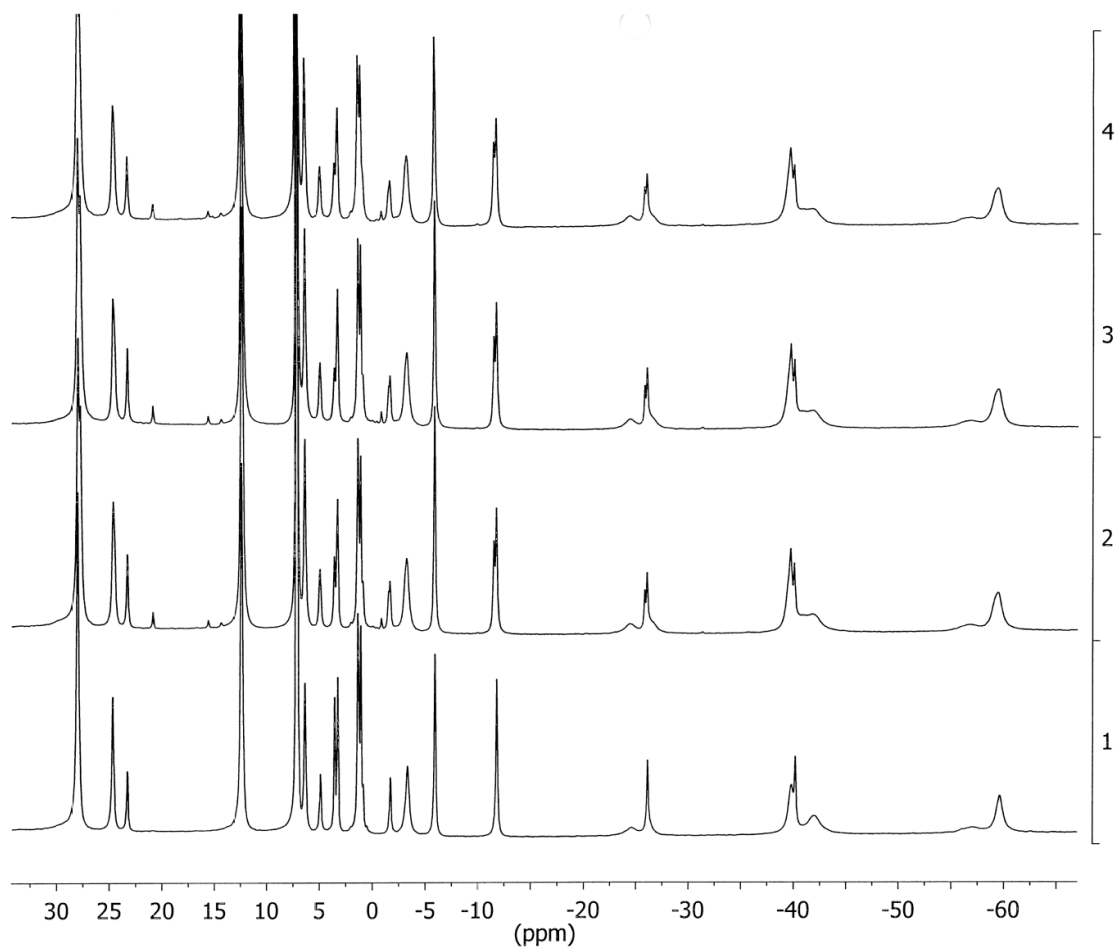


Figure S-6. ^1H NMR spectra of cobalt(II) hydride complexes. Spectrum 1 is $[\text{L}^{\text{tBu}}\text{Co}(\mu\text{-D})]_2$, prepared from Et_3SiD as described in the text. Spectrum 2 is the same tube after addition of ~ 1 equiv of $[\text{L}^{\text{tBu}}\text{Co}(\mu\text{-H})]_2$, in which the PIECS in the peaks at δ -12, -26, and -40 ppm is visible. Spectrum 3 was taken after 6 h at room temperature, and spectrum 4 after 12 h at 60 $^\circ\text{C}$. There is no change in the spectra, indicating a lack of isotope exchange which would form the mixed H/D isomer.

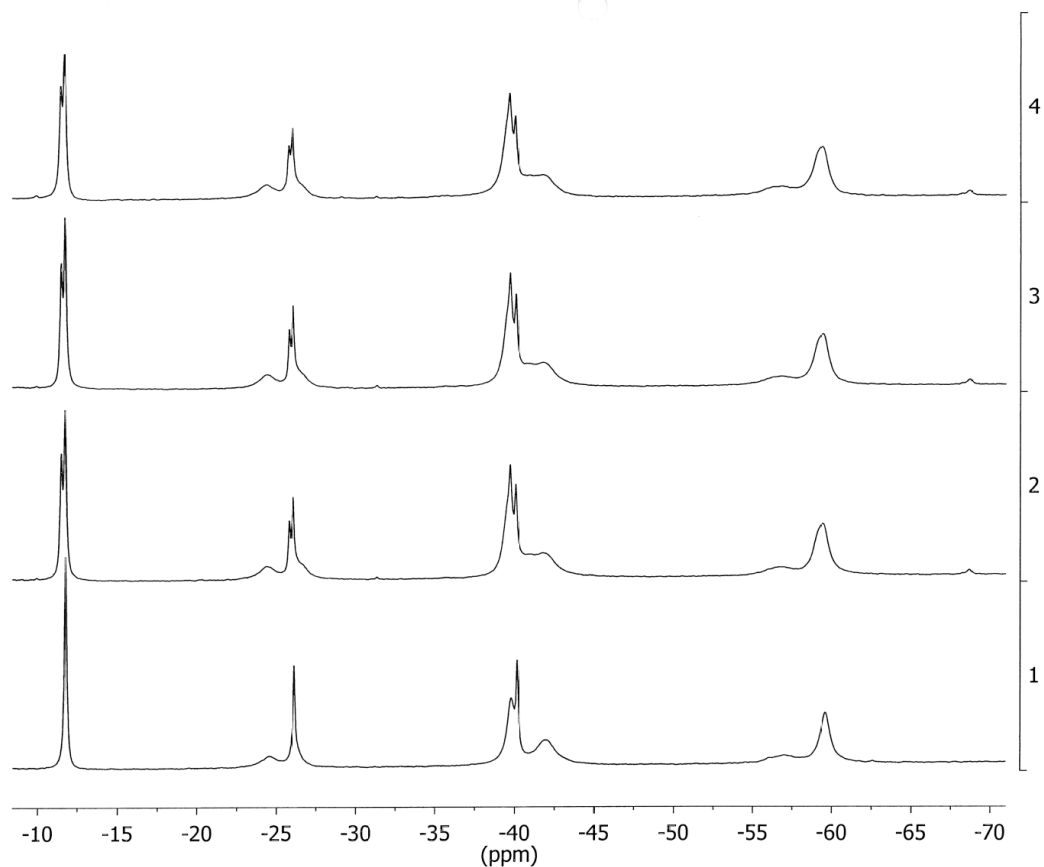


Figure S-7. Close-up of one region of the spectra in Figure S-6.

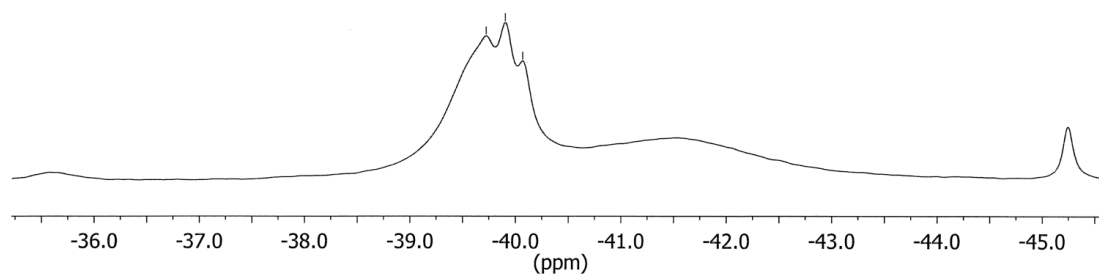


Figure S-8. Independent preparation of a mixture of $[\text{L}^{\text{tBu}}\text{Co}(\mu\text{-D})]_2$, $\{\text{L}^{\text{tBu}}\text{Co}\}_2(\mu\text{-H})(\mu\text{-D})$, and $[\text{L}^{\text{tBu}}\text{Co}(\mu\text{-H})]_2$ (by using a 1:1 mixture of Et_3SiH and Et_3SiD in the preparation of the hydride complex) shows that the mixed-label $\{\text{L}^{\text{tBu}}\text{Co}\}_2(\mu\text{-H})(\mu\text{-D})$ peaks are distinguishable from the two isotopologues. Therefore, if the mixed-label compound had been formed in the experiment described in Figure S-6, then it would have been observable.

X-ray Crystallography. A crystal of $L^{Mc}FeBr(THF)$ (**2**) ($0.36 \times 0.32 \times 0.26 \text{ mm}^3$) was placed onto the tip of a 0.1 mm diameter glass capillary tube or fiber and mounted on a Bruker SMART APEX II CCD Platform diffractometer for a data collection at 100.0(1) K.ⁱ A preliminary set of cell constants and an orientation matrix were calculated from reflections harvested from three orthogonal wedges of reciprocal space. The full data collection was carried out using MoKa radiation (graphite monochromator) with a frame time of 30 seconds and a detector distance of 4.97 cm. A randomly oriented region of reciprocal space was surveyed: four major sections of frames were collected with 0.50° steps in ω at four different ϕ settings and a detector position of -33° in 2θ . The intensity data were corrected for absorption.ⁱⁱ Final cell constants were calculated from the xyz centroids of 3900 strong reflections from the actual data collection after integration.ⁱⁱⁱ

The structure was solved using SIR97^{iv} and refined using SHELXL-97.^v The space group $P2_1/n$ was determined based on systematic absences and intensity statistics. A direct-methods solution was calculated which provided most non-hydrogen atoms from the E-map. Full-matrix least squares / difference Fourier cycles were performed which located the remaining non-hydrogen atoms. All non-hydrogen atoms were refined with anisotropic displacement parameters. All hydrogen atoms were placed in ideal positions and refined as riding atoms with relative isotropic displacement parameters. The refinement stalled at $R1 = 0.0757$, at which point twin modeling was required. After the non-merohedral twin law, $[1\ 0\ 0 / 0\ -1\ 0 / -0.259\ 0\ -1]$, a 180° rotation about direct lattice $[1\ 0\ 0]$, was determined,^{vi} the data were re-integrated,ⁱⁱⁱ and a new absorption correction was applied.^{vii} There were 8902 unique reflections associated solely with one component, 8801 unique reflections associated solely with the second component, and 9493 unique overlapping reflections. The ratio of the two components refined to 87:13. The final full matrix least squares refinement converged to $R1 = 0.0531$ (F^2 , $I > 2\sigma(I)$) and $wR2 = 0.1340$ (F^2 , all data).

Table S-1. Details of X-ray crystal structure of L^{Me}FeBr(THF).

Empirical formula	C ₃₃ H ₄₉ N ₂ FeBrO
FW	625.50
Crystal system	Monoclinic
Space group	<i>P2₁/n</i>
<i>a</i> (Å)	10.154(3)
<i>b</i> (Å)	14.784(4)
<i>c</i> (Å)	21.700(6)
α (deg)	90
β (deg)	93.489(4)
γ (deg)	90
<i>V</i> (Å ³)	3251.5(14)
<i>Z</i>	4
ρ (g/cm ³)	1.278
μ (mm ⁻¹)	1.719
<i>R</i> 1, <i>wR</i> 2 (<i>I</i> > 2σ(<i>I</i>))	0.0531, 0.1301
<i>R</i> 1, <i>wR</i> 2 (all data)	0.0689, 0.1340
GOF	1.160

ⁱ *APEX2*, version 2009.9-0; Bruker AXS: Madison, WI, 2009.

ⁱⁱ Sheldrick, G. M. *SADABS*, version 2008/1; University of Göttingen: Göttingen, Germany, 2008.

ⁱⁱⁱ *SAINT*, version 7.68A; Bruker AXS: Madison, WI, 2009.

^{iv} Altomare, A.; Burla, M. C.; Camalli, M.; Casciarano, G. L.; Giacovazzo, C.; Guagliardi, A.; Moliterni, A. G. G.; Polidori, G.; Spagna, R. *SIR97: A new program for solving and refining crystal structures*; Istituto di Cristallografia, CNR: Bari, Italy, 1999.

^v Sheldrick, G. M. *Acta. Cryst.* **2008**, *A64*, 112-122.

^{vi} (a) Parsons, S.; Gould, B.; Cooper, R.; Farrugia, L. *ROTAX*; University of Edinburgh: Edinburgh, Scotland, 2003; (b) Sheldrick, G. M. *CELL_NOW*, version 2008/2; University of Göttingen: Göttingen, Germany, 2008.

^{vii} Sheldrick, G. M. *TWINABS*, version 2008/4; University of Göttingen: Göttingen, DE, 2008.